JOURNAL OF COMPUTATIONAL PHYSICS 87, 47–60 (1990)

An Explicit Finite-Difference Solution to the Wave Equation with Variable Velocity

ALVIN K. BENSON

Department of Geology and Geophysics, Brigham Young University, Provo, Utah 84602

Received August 12, 1988; revised March 8, 1989

An explicit method is formulated for solving the scalar wave equation using finite differences in isotropic, inhomogeneous media. Extrapolation from the known grid-plane to the unknown grid-plane is in *depth* so that the final result represents an image of the medium's true spatial structure. This image is often used to predict favorable locations for drilling into the earth. This paper determines equations for the depth differencing coefficients and the lateral differencing coefficients of a polynomial series solution to the wave equation.

INTRODUCTION

Solving the scalar wave equation in isotropic, inhomogeneous media is fundamental in the study of seismology. Several methods have been developed to solve this problem. Among these are the reflectivity method [1], the generalized ray method [2], the ray series method [3, 4], finite-element methods [5–7], and finite-difference methods [8–14].

Using finite differences, the scalar wave equation can be solved explicitly or implicitly. Starting from a number of data points in the known (data acquisition) plane, the explicit method determines information about one point in the unknown plane, whereas the implicit method generates coupled information about a number of points in the unknown plane. The coupled information must be unscrambled by a matrix inversion in order to determine specific values at each point in the unknown plane [15]. Stable explicit methods are much cheaper (3 to 6 times) than implicit methods. This paper deals with an explicit finite-difference solution to the scalar wave equation with variable velocity.

FORMULATION OF THE PROBLEM

When a geophysical problem is described by the wave equation, solution usually involves extrapolating wavefields in time or depth. The procedure depends on how we express the partial derivatives of the upward and downward propagating waves. Modeling implies the extrapolation of waves *forward* in time or depth through a

0021-9991/90 $3.00

581/87/1-4

given velocity structure. Migration is the inverse of this procedure, extrapolation of recorded wavefields *backward* in time or depth through an estimated velocity structure. I will consider the inverse problem in this paper. The forward problem can be formulated from this solution by changing all the signs in front of the depth z to the opposite sign.

Let us start with a recorded wavefield $R(x, z, t)$, which could represent pressure, displacement, etc., and which obeys the two-dimensional scalar wave equation

$$R_{xx} + R_{zz} - \frac{4}{v^2(x, z)} R_{tt} = 0, \tag{1}$$

where the subscripts denote partial derivatives. The factor of 4 comes from applying the exploding reflector model. Although a stacked seismic section is produced by the upward reflection and diffraction of originally downgoing waves, simplistic considerations permit us to visualize it as a superposition of just upward traveling waves. This is done by making the following two assumptions: (1) replace the travel path from source to reflector to receiver with a travel path from reflector to receiver only and (2) replace the medium velocity v by $v/2$. The velocity is a function of x and z. The time coordinate is Fourier transformed to angular frequency, so that

$$R(x, z, t) \rightarrow R(x, z, \omega), \tag{2}$$

where $R(x, z, \omega)$ obeys the equation

$$R_{xx} + R_{zz} + \frac{4\omega^2}{v^2} R = 0. \tag{3}$$

The main advantages of transforming to frequency are (a) each frequency can be propagated separately, which can simplify analysis of large data sets and (b) time shifts over noninteger numbers of sampling intervals and all time derivatives are replaced by simple multiplications.

A coordinate transformation to a retarded time frame is then invoked [16] in order to slow R down, by defining

$$Q(x, z, \omega) \equiv R(x, z, \omega)\, e^{+i(2\omega z/\bar{v})}, \tag{4}$$

where $\bar{v}$ is some average velocity which is determined from the velocity structure. This average velocity is calculated by breaking the assumed interval velocity model into blocks in the x and z directions and determining an average velocity in each block by summing the interval velocities at all grid points in the block and dividing by the total number. Block size can vary from data set to data set, but a typical size might be 5000 ft laterally by 2000 ft vertically. Q obeys the equation

$$Q_{xx} + \omega^2 SQ - \frac{4i\omega}{\bar{v}} Q_z + Q_{zz} = 0, \tag{5}$$

where S is given by

$$S = \frac{4}{v^2} - \frac{4}{\bar{v}^2}, \tag{6}$$

and is called the slowness function. Many times in finite difference approximations, the assumption of locally constant coefficients is made by setting $v = \bar{v}$ in Eq. (5). I will not make this approximation. In fact, at this point, no approximations to Eq. (1) have been made. Equation (5) is simply the scalar wave equation in a shifted coordinate system.

The solution to Eq. (5) now involves two problems:

(a) differencing in depth z and

(b) differencing in lateral coordinate x.

Differencing in Z

Rearranging Eq. (5) gives

$$Q_{xx} + \omega^2 S Q = + \frac{4i\omega}{\bar{v}} Q_z - Q_{zz}. \tag{7}$$

Equation (7) relates the operator

$$\zeta = \partial_x^2 + \omega^2 S(x, z) \tag{8}$$

to the first and second z-derivatives of Q. For a finite change in *depth* Δz the form of Eq. (7) suggests trying a polynomial series approximation solution of the form

$$\bar{Q}(x, z + \Delta z, \omega) = \sum_{m=0}^{M} C_m (\partial_x^2 + \omega^2 S)^m (\Delta x)^{2m} Q(x, z, \omega). \tag{9}$$

The c_m's are complex numbers to be determined, assuming that v is not equal to $\bar{v}$.

To determine the c's, let us compare the solution in Eq. (9) to an upcoming plane wave solution to Eq. (5) given by

$$Q(x, \Delta z, \omega) = Q(x, 0, \omega) \exp\left\{ -i \left[\frac{2\omega \Delta z}{\bar{v}} \right] \left[\left(\frac{\bar{v}}{v} \right) \sqrt{1 - \frac{k_x^2 v^2}{4\omega^2}} - 1 \right] \right\}, \tag{10}$$

where $k_x^2 Q = -\partial_x^2 Q$. This solution can be verified by running it through Eq. (5). It is valid if $v =$ constant for a given local area of interest.

Defining a dip angle α by

$$\sin \alpha \equiv \frac{k_x v}{2\omega} \tag{11}$$

and a dimensionless quantity γ by

$$\gamma \equiv \frac{2\omega \Delta z}{\bar{v}}, \tag{12}$$

Eq. (9) and (10) become, respectively,

$$\bar{Q}(x, z+\Delta z, \omega) = \sum_{m=0}^{M} C_m \left(\frac{\gamma \Delta x}{\Delta z}\right)^{2m} \left[\left(\frac{\bar{v}}{v}\cos\alpha\right)^2 - 1\right]^m Q(x, z, \omega) \tag{13}$$

and

$$Q(x, z+\Delta z, \omega) = \exp i\left[-\gamma\left(\frac{\bar{v}}{v}\cos\alpha - 1\right)\right] Q(x, z, \omega). \tag{14}$$

A "best" set of c's can now be determined by minimizing the least squares error between $\bar{Q}$ and Q over the physical range of dips and velocities. Defining

$$\mu \equiv \frac{\bar{v}}{v}\cos\alpha, \tag{15}$$

the problem reduces to minimizing the difference between

$$\bar{Q} = \sum_{m=0}^{M} C_m \left(\frac{\gamma \Delta x}{\Delta z}\right)^{2m} (\mu^2 - 1)^m \tag{16}$$

and

$$Q = \exp i[-\gamma(\mu - 1)], \tag{17}$$

over an expected physical range of μ.

The Coefficients

Due to (a) spatial averaging resulting from an *area* source vs a point source and receiver *arrays* vs points and (b) finite spacing producing sampling rate problems, a reasonable limit on dips α might be from $-55°$ to $+55°$. Lateral velocity variations may be on the order of 2:1, such as in the Wyoming overthrust belt, where velocities can go from 10,000 ft/s in sedimentary rocks to 20,000 ft/s in granite. Vertical variations may be on the order of 4:1, such as going from water at 5000 ft/s to quartz at 20,000 ft/s. These physical limits yield the limits on μ so that the minimization between $\bar{Q}$ and Q can be carried out.

A reasonable range might be

$$0.7 < \frac{\bar{v}}{v} < 1.4. \tag{18}$$

Since

$$\mu = \frac{\bar{v}}{v}\cos\alpha = \frac{\bar{v}}{v}\sqrt{1 - k_x^2 v^2/4\omega^2}, \tag{19}$$

then

$$\mu = \begin{cases} \dfrac{\bar{v}}{v}\sqrt{1 - k_x^2 v^2/4\omega^2} & \left(\text{for } \dfrac{k_x v}{2\omega} < 1\right) \\ i\dfrac{\bar{v}}{v}\sqrt{k_x^2 v^2/4\omega^2 - 1} & \left(\text{for } \dfrac{k_x v}{2\omega} > 1\right), \end{cases} \tag{20}$$

where k_x varies over the range $(0, \pi/\Delta x)$. The maximum value of μ will be

$$\mu_{\max} = \frac{\bar{v}}{v_{\min}} \equiv \mu_f, \tag{21}$$

where $v_{\min}$ is the minimum velocity for a given region of interest.

The minimum value of μ will be

$$\mu_{\min} = \frac{\bar{v}}{v_{\max}}\cos\theta_{\max}, \tag{22}$$

where $\theta_{\max}$ is the maximum dip in the data. If $\pi v/\omega\Delta x > 1$, μ takes on imaginary values. Defining $\mu = iv$, the maximum v will be

$$v_f \equiv v_{\max} = \frac{\bar{v}}{v}\sqrt{\frac{\pi^2 v^2}{\omega^2 \Delta x^2} - 1}. \tag{23}$$

Consequently, the problem of determining the c's boils down to fitting $\bar{Q}$ to $\exp i[\quad -\gamma(\mu - 1)]$ in the region of real μ and to $\exp(+i\gamma)\exp(+\gamma v)$ in the region of imaginary μ.

Choosing a weighted least squares fit of $\bar{Q}$ to Q and defining the real and imaginary parts of c_m in the following manner,

$$C'_m \equiv [a_m + ib_m] \cdot \left(\frac{\gamma\Delta x}{\Delta z}\right)^{2m}, \tag{24}$$

separate expressions can be written for the least squares error of the real and imaginary parts of $\bar{Q} - Q$:

$$\varepsilon_1 = \int_0^{\mu_f} d\mu\lambda_1(\mu)\,|\mathrm{Re}(\bar{Q} - Q)|^2 + \int_0^{v_f} dv\lambda_2\,|\mathrm{Re}(\bar{Q} - Q)|^2 \tag{25}$$

$$\varepsilon_2 = \int_0^{\mu_f} d\mu\lambda_1(\mu)\,|\mathrm{Im}(\bar{Q} - Q)|^2 + \int_0^{v_f} dv\lambda_2(v)\,|\mathrm{Im}(\bar{Q} - Q)|^2, \tag{26}$$

where λ_1 and λ_2 are weighting functions which should be high for real μ, the region of greatest interest. For imaginary μ and $\mu < \mu_{\min} \neq 0$, λ can be chosen just large enough so that

$$\operatorname{Max}|\bar{Q}|^2 \leqslant 1, \tag{27}$$

where

$$|\bar{Q}|^2 = \bar{Q}\bar{Q}^*. \tag{28}$$

Equation (27) is a stability criteria to assure that energy does not grow. Treating ε_1 first,

$$\varepsilon_1 = \int_0^{\mu_f} d\mu \lambda_1(\mu) \left| \sum_m a_m(\mu^2 - 1)^m - \cos \gamma(\mu - 1) \right|^2 + \int_0^{\nu_f} d\nu \lambda_2(\nu) \left| \sum_m a_m(-1)^m (\nu^2 + 1)^m - \cos \gamma \, e^{+\gamma\nu} \right|^2 \tag{29}$$

and

$$\frac{\partial \varepsilon_1}{\partial a_m} = \int_0^{\mu_f} d\mu \lambda_1(\mu)(\mu^2 - 1)^m \left(\sum_{m'} a_{m'}(\mu^2 - 1)^{m'} - \cos \gamma(\mu - 1) \right) + (-1)^m \int_0^{\nu_f} d\nu \lambda_2(\nu)(\nu^2 + 1)^m \left(\sum_{m'} a_{m'}(-1)^{m'} (\nu^2 + 1)^{m'} - \cos \gamma \, e^{+\gamma\nu} \right). \tag{30}$$

Setting the partial derivative of ε_1 to zero yields

$$\sum_{m'} a_{m'} \left[\int_0^{\mu_f} \lambda_1(\mu)(\mu^2 - 1)^{m+m'} d\mu + (-1)^{m+m'} \int_0^{\nu_f} d\nu \lambda_2(\nu)(\nu^2 + 1)^{m+m'} \right] = \left[\int_0^{\mu_f} d\mu \lambda_1(\mu)(\mu^2 - 1)^m \cos \gamma(\mu - 1) + (-1)^m \int_0^{\nu_f} d\nu \lambda_2(\nu)(\nu^2 + 1)^m \cos \gamma \, e^{+\gamma\nu} \right]. \tag{31}$$

In an analagous manner,

$$\varepsilon_2 = \int_0^{\mu_f} d\mu \lambda_1(\mu) \left| \sum_m b_m(\mu^2 - 1)^m + \sin \gamma(\mu - 1) \right|^2 + \int_0^{\nu_f} d\nu \lambda_2(\nu) \left| \sum_m b_m(-1)^m (\nu^2 + 1)^m - \sin \gamma \, e^{+\gamma\nu} \right|^2 \tag{32}$$

and

$$\frac{\partial \varepsilon_2}{\partial b_m} = \left[\int_0^{\mu_f} d\mu \lambda_1(\mu)(\mu^2-1)^m \left(\sum_{m'} b_{m'}(\mu^2-1)^{m'} + \sin\gamma(\mu-1) \right) \right.$$
$$\left. + (-1)^m \int_0^{v_f} dv \lambda_2(v)(v^2+1)^m \left(\sum_{m'} b_{m'}(v^2+1)^{m'} - (-1)^{m'} \sin\gamma\, e^{+\gamma v} \right) \right]. \quad (33)$$

Setting Eq. (33) equal to zero, the following expression is obtained for the b_m's:

$$\sum_{m'} b_{m'} \left[\int_0^{\mu_f} d\mu \lambda_1(\mu)(\mu^2-1)^{m+m'} + (-1)^{m+m'} \int_0^{v_f} dv \lambda_2(v)(v^2+1)^{m+m'} \right]$$
$$= -\left[\int_0^{\mu_f} d\mu \lambda_1(\mu)(\mu^2-1)^m \sin\gamma(\mu-1) \right.$$
$$\left. - (-1)^m \int_0^{v_f} dv \lambda_2(v)(v^2+1)^m \sin\gamma \cdot e^{+\gamma v} \right]. \quad (34)$$

Equations (31) and (34) can be solved using Simpson's rule to evaluate the integrals and then using a matrix inversion algorithm to solve for the a's and the b's. This inversion is very fast, since 2–4 m's should be sufficient.

Differencing in X

A finite difference approximation is needed for the operators

$$\hat{\zeta}^m = (\partial_x^2 + \omega^2 S(x,z))^m \quad (35)$$

which appear in Eq. (9). One way to do this is to approximate $\hat{\zeta}$ by a $2L+1$ point filter. Using the notation

$$\hat{\zeta} \approx \bar{\zeta}, \qquad Q(j\Delta x) \approx Q_j, \quad (36)$$

we will define

$$(\hat{\zeta} Q)_j \equiv \sum_{l=-L}^{L} \bar{\zeta}_l Q_{j+l}. \quad (37)$$

Thus, $\hat{\zeta}^m Q$ is represented by applying the filter $\bar{\zeta}$ m times.

Now let us concentrate on $\partial_x^2 Q$ and find a $2L+1$ approximation for it. Defining

$$(\Delta_l^2 Q)_j \equiv Q_{j+l} - 2Q_j + Q_{j-l}. \quad (38)$$

we approximate the lateral second derivative with a polynomial series expansion

$$\bar{d}_j^2 Q \equiv \frac{1}{(\Delta x)^2} \sum_{l=1}^{L} b_l (\Delta_l^2 Q)_j. \quad (39)$$

To help find the $\bar{d}^2$ that "best" approximates ∂_x^2, let us determine the coefficients b_l when Q is chosen as a plane wave solution in Eq. (39). Selecting $Q = e^{iPx}$, Eq. (39) becomes

$$(\bar{d}^2 Q) = \frac{-4}{(\Delta x)^2} \sum_{l=1}^{L} b_l \sin^2\left(\frac{lP\Delta x}{2}\right), \tag{40}$$

where P is used to represent the horizontal wave number. But also,

$$\partial_x^2 Q = -P^2 Q. \tag{41}$$

Consequently, the "best" values for b_l are those which satisfy the equation

$$\sum_{l=1}^{L} b_l \sin^2\left(\frac{lP\Delta x}{2}\right) \approx \frac{P^2 \Delta x^2}{4}, \tag{42}$$

over the acceptable values of P. Good choices to try for L might be 3, 5, 7, etc.

The Lateral Coefficients

Choosing a least squares fit of Eq. (40) to Eq. (41), to determine the lateral coefficients (the b's), a number of choices are available in making the fit. Three will be considered in this paper.

The first attempt is a straightforward, unconstrained least squares fit up to the Nyquist wavenumber, $P_N = \pi/\Delta x$. We want to minimize the integral E,

$$E = \int_0^{P_N} \left| \frac{P^2 \Delta x^2}{4} - \sum_{l=1}^{L} b_l \sin^2\left(\frac{lP\Delta x}{2}\right) \right|^2 dP \tag{43}$$

with respect to the b's. This yields

$$\frac{\partial E}{\partial b_j} = \frac{\pi}{j^2 \Delta x}(-1)^j - \frac{\pi^3}{6\Delta x} + \sum_{l=1}^{L} \frac{4b_l}{\Delta x}\left(\frac{1}{4}\pi + \frac{1}{4}\frac{\pi \delta_{jl}}{2}\right). \tag{44}$$

Upon setting Eq. (44) to zero, the equation to solve for the b's is

$$\sum_{l=1}^{L} b_l (1 + \delta_{jl}/2) = \frac{\pi^2}{6} - \frac{(-1)^j}{j^2}. \tag{45}$$

Tests on a variety of models have shown that for much lateral variation in the velocity v in Eq. (1), this set of b's produces instabilities.

The second attempt tried was a constrained least squares fit taking $\bar{d}^2 = P^2$ up to some P_F, and then equal to P_F^2 up to the Nyquist wavenumber, P_N. This fit is

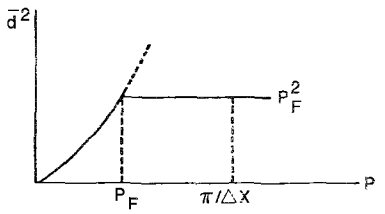

FIG. 1. A constrained least squares fit for the second lateral derivative.

shown graphically in Fig. 1. The functional E to minimize with respect to the b's for this case is

$$E=\int_0^{P_F}\left|\frac{P^2(\Delta x)^2}{4}-\sum_{l=1}^{L} b_l \sin^2\left(\frac{lP\Delta x}{2}\right)\right|^2 dP + \int_{P_F}^{\pi/\Delta x} dP\left|\frac{P_F^2\Delta x^2}{4}-\sum_{l=1}^{L} b_l \sin^2\left(\frac{lP\Delta x}{2}\right)\right|^2. \tag{46}$$

The resulting equation to solve for the b's is given by

$$\sum_l b_l\left(1+\frac{\delta_{jl}}{2}\right)=\frac{1}{\pi}\left(-\frac{\theta^3}{3}+\frac{1}{j^3}\sin(j\theta)+\frac{1}{2}\theta^2\pi-\frac{\theta\cos(j\theta)}{j^2}\right), \tag{47}$$

where $\theta=P_F\Delta x$. This again is not a good fit, generating instabilities when there is much lateral variation in velocity.

The third choice is a constrained least squares fit taking $\bar{d}^2=P^2$ up to some P_F, and then fitting it to a quadratic out to P_N. This fit is illustrated in Fig. 2. The functional to minimize is

$$E=\int_0^{P_F}\left|\frac{(P\Delta x)^2}{4}-\sum_{l=1}^{L} b_l \sin^2\left(\frac{lP\Delta x}{2}\right)\right|^2 dP + \int_{P_F}^{\pi/\Delta x} dP\left|f(P)-\sum_{l=1}^{L} b_l \sin^2\left(\frac{lP\Delta x}{2}\right)\right|^2, \tag{48}$$

where $f(P)$ is a quadratic function to be determined. The conditions chosen to

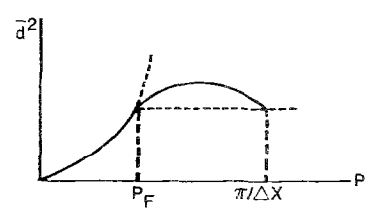

FIG. 2. The chosen constrained least squares fit for the second lateral derivative.

determine $f(P)$ are (a) its first derivative at P_N is zero, and (b) $f(P_F)=P_F^2$ for some P_F as shown in Fig. 2. From these conditions $f(P)$ is found to be

$$f(P)=P_F^2+2P_F(P-P_F)+\left(\frac{P_F}{P_F-\pi/\Delta x}\right)(P-P_F)^2.$$

Upon minimization of E w.r.t. the b's in a least squares sense, we have

$$\sum_l b_l\left(1+\frac{\delta_{lj}}{2}\right)=\begin{cases}-\dfrac{1}{j^2}+\dfrac{P\Delta x}{3}\left(\pi-\dfrac{P\Delta x}{2}\right) & \text{if } j \text{ is even}\\ +\dfrac{1}{j^2}+\dfrac{P\Delta x}{3}\left(\pi-\dfrac{P\Delta x}{2}\right) & \text{if } j \text{ is odd,}\end{cases} \tag{49}$$

which has provided a stable fit for all tested cases.

Examples

From the explicit polynomial series solution in Eqs. (9) and (13) and the transformation in Eq. (4), a solution to the inverse problem (migration) can be immediately written down. The final migrated geophysical data are given by the explicit formula

$$R(x,z,0)=\sum_{m,\omega} C'_m\left[\sum_k D(k)+\left(\frac{\bar{v}^2}{v^2}-1\right)\right]^m e^{-i\omega 2z\cdot\bar{v}}\,R(x,o,\omega), \tag{50}$$

(x—2nd difference operator)

Migrated section; (z-Differencing coefficients); (Variable velocity $v(x,z)$); (Downward continuation operator); (Record section)

where c'_m is found from Eqs. (24), (31), and (34). $D(k)$ is the finite difference approximation to the second derivative operator in x and is given by Eqs. (39) and (49).

The migrated data, $R(x, z, t=0)$, represent reflection coefficients at boundaries of velocity and/or density contrasts. This reflectivity function is obtained explicitly from the acquired surface data, $R(x, z=0, t)$, by the transformation in Eq. (50). A computer algorithm to generate the solution in Eq. (50) would proceed as follows:

a. Take the known record field, $R(x, 0, t)$ and Fourier transform it: $R(x, 0, t)\rightarrow R(x, 0, \omega)$. Note that $Q(x, o, \omega)=R(x, o, \omega)$.

b. Transpose R into arrays of constant ω (for all x and given z).

c. Transpose $S(x, z)$ into arrays of constant z (for all x).

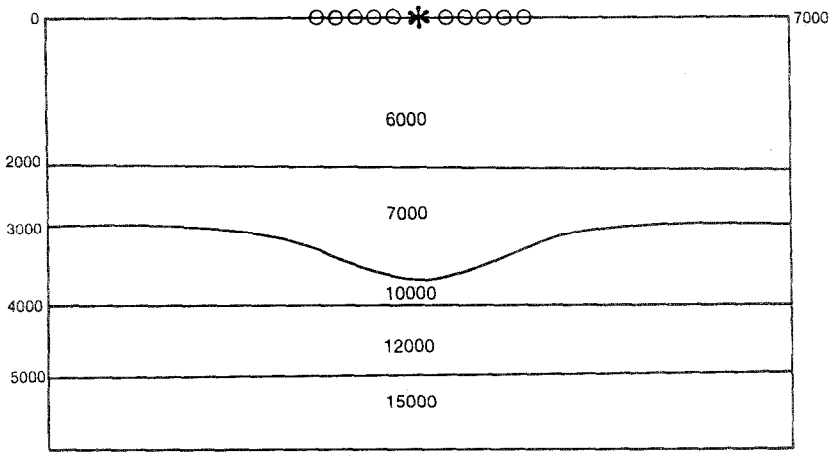

FIG. 3. Syncline (valley) model.

d. For each $\omega \leqslant \omega_{max}$, continue downward 1 z-step, using Eq. (50). Continue if $z < z_{bottom}$, until finished.

e. Transpose the migrated section into arrays of constant x.

f. Final result is a migrated depth section.

Figure 3 shows a classical earth cross section of a syncline (concave curvature) with a flat layer above and two flat layers below. Variations in velocity are primarily vertical, going from 6000 ft/s shallow to 15,000 ft/s deep, with lateral variations across the syncline, from 7000 to 10,000 ft/s.

The data in Fig. 4 were generated using a ray tracing algorithm. This represents synthetic surface seismic data acquired by setting off a source and recording the

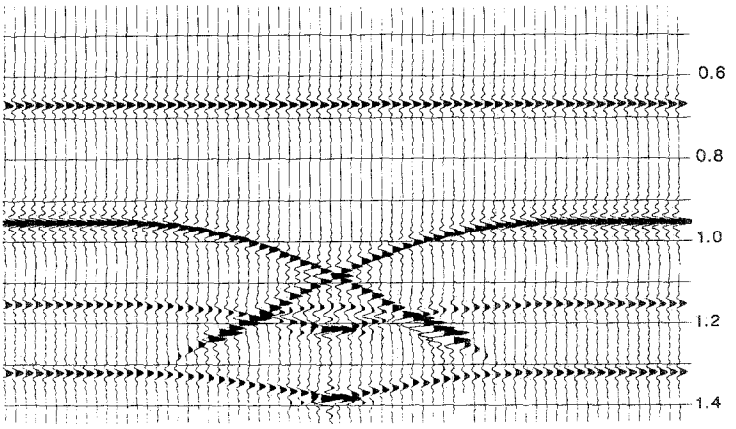

FIG. 4. Synthetic surface data from the syncline model.

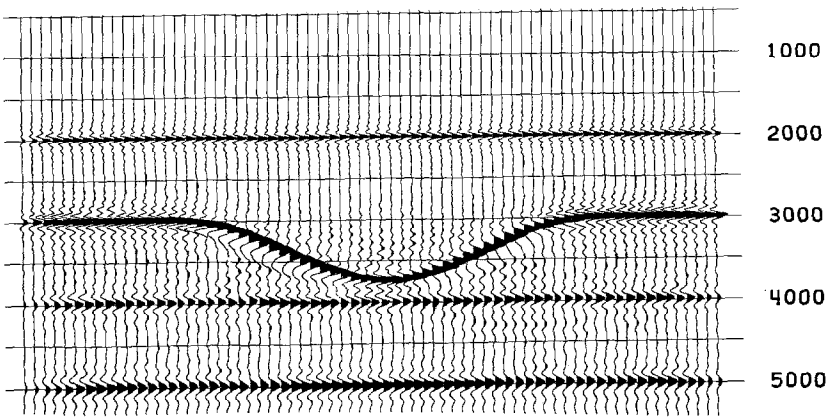

FIG. 5. Reconstructed syncline model using the explicit finite difference solution to the wave equation.

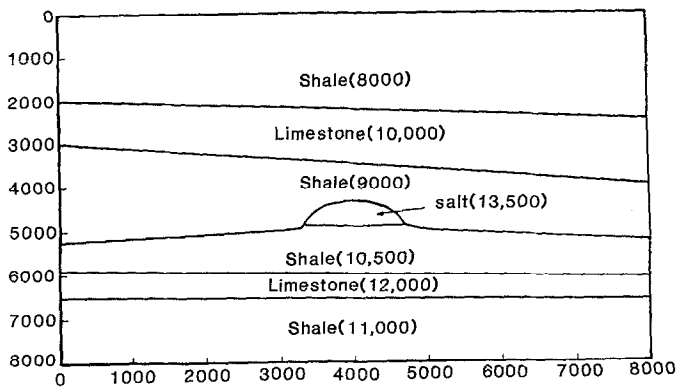

FIG. 6. Dome model.

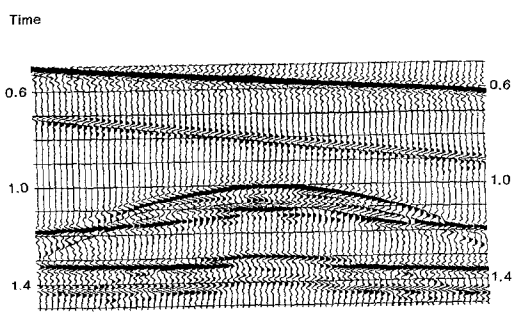

FIG. 7. Synthetic surface data from the dome model.

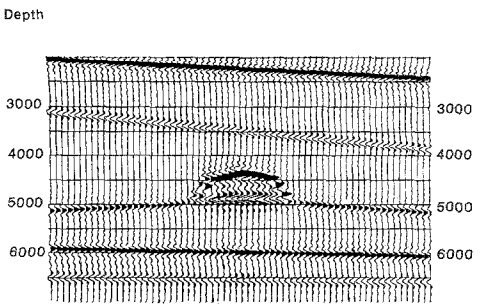

FIG. 8. Reconstructed dome model using the explicit finite difference solution to the wave equation.

primary reflected energy in receivers collocated with the source. It shows the characteristic "bow-tie" effect for a syncline and also velocity pull-down in the layers underneath. Running the above algorithm on this simulated data set essentially recovers the original model, except for some areas of dispersion, as shown in Fig. 5.

The second model, shown in Fig. 6, is an anticline (dome) with dipping layers above and below the dome. Vertical velocity variations are rapid, as are lateral variations across the dome, ranging from 9000 to 14,000 ft/s. The collocated synthetic data in Fig. 7 were generated by a wave equation modelling program. Notice how the dome is diffracted and spread out as seen at the surface. Also, note the velocity pull-up of the underneath layers.

Running the above algorithm on the data set in Fig. 7 reconstructs a very good representation of the original model, as shown in Fig. 8. The dome has been effectively collapsed back to its original self, and the lower dipping layers have been imaged into their correct positions with excellent continuity.

CONCLUSIONS

An explicit finite difference polynomial series solution (Eq. (9)) to the wave equation has been formulated, and the depth and lateral differencing coefficients determined. Equation (9) can be made an arbitrarily good estimate of Q provided derivatives of velocity are small, and this is usually the assumption even in very sophisticated depth migration schemes [15]. The reflectivity function can be formed from this solution as shown in Eq. (50). As demonstrated by two examples, the solution works in inhomogeneous media where velocity changes rapidly both vertically and laterally.

ACKNOWLEDGMENT

The author extends appreciation to R. H. Stolt for many informative discussions and insights.

REFERENCES

1. K. FUCHS AND G. MULLER, *Geophys. J. Roy. Astron. Soc.* **23**, 417 (1971).
2. D. V. HELMBERGER, *SSA Bull.* **58**, 179 (1968).
3. V. CERVENY, I. A. MOLOTKOV, AND I. PSENCIK, *The Ray Method in Seismology* (Charles University Press, Prague, 1978).
4. F. C. KARAL, JR. AND J. B. KELLER, *J. Acoust. Soc. Amer.* **31**, 694 (1959).
5. W. D. SMITH, *Geophys. J. Roy. Astron. Soc.* **42**, 747 (1975).
6. W. D. SMITH AND B. A. BOLT, *Geophys. J. Roy. Astron. Soc.* **45**, 647 (1976).
7. W. C. THACKER, *J. Phys. Ocean.* **8**, 680 (1978).
8. Z. S. ALTHERMAN AND F. C. KARAL, JR., *SSA Bull.* **58**, 367 (1968).
9. D. M. BOORE, *Finite-Difference Methods For Seismic Wave Propagation in Heterogeneous Materials in Methods in Computational Physics*, Vol. II, edited by B. Alder, S. Fernback, and M. Rotenberg, (Academic Press, New York, 1972).
10. R. M. ALFORD, K. R. KELLY, AND D. M. BOORE, *Geophysics* **39**, 834 (1974).
11. K. R. KELLY, R. W. WARD, S. TREITEL, AND R. M. ALFORD, *Geophysics* **41**, 2 (1976).
12. J. GAZDAG, *Geophys. Prospect.* **28**, 60 (1980).
13. A. J. BERKHOUT, *Seismic Migration—Imaging of Acoustic Energy by Wave Field Extrapolation* (Elsevier, Amsterdam, 1980).
14. E. KJARTANSSON, Ph. D. thesis, Stanford Exploration Project Report No. 23, Stanford University, 1979 (unpublished).
15. R. H. STOLT AND A. K. BENSON, *Seismic Migration: Theory and Practice* (Geophysical Press, Amsterdam, 1986).
16. J. CLAERBOUT, *Fundamentals of Geophysical Data Processing* (McGraw–Hill, New York, 1976).